European Journal of Medicinal Chemistry 183 (2019) 111686

Contents lists available at ScienceDirect

European Journal of Medicinal Chemistry

journal homepage: http://www.elsevier.com/locate/ejmech

Research paper

Two optimized antimicrobial peptides with therapeutic potential for clinical antibiotic-resistant *Staphylococcus aureus*

Chunlei Li [a, b, 1], Chengguang Zhu [c, d, 1], Biao Ren [c], Xin Yin [a], Sang Hee Shim [e], Yue Gao [b], Jianhua Zhu [b], Peipei Zhao [a], Changheng Liu [a], Rongmin Yu [b, **], Xuekui Xia [a, *], Lixin Zhang [a, f, ***]

[a] Key Biosensor Laboratory of Shandong Provinde, Biology Institute, Qilu University of Technology (Shandong Academy of Sciences), Jinan, 250103, China
[b] Biotechnological Institute of Chinese Materia Medica, Jinan University, 601 Huangpu Avenue West, Guangzhou, 510632, China
[c] State Key Laboratory of Oral Diseases, Sichuan University, Chengdu, 610041, China
[d] Department of Operative Dentistry and Endodontics, West China Hospital of Stomatology, Sichuan University, Chengdu, 610041, China
[e] College of Pharmacy and Innovative Drug Center, Duksung Women's University, Seoul, 01369, South Korea
[f] State Key Laboratory of Bioreactor Engineering, East China University of Science and Technology, Shanghai, 200237, China

ARTICLE INFO

Article history:
Received 6 May 2019
Received in revised form
25 August 2019
Accepted 6 September 2019
Available online 7 September 2019

Keywords:
Optimized antimicrobial peptide
Anti-MRSA
Anti-biofilm
SEM
qRT-PCR

ABSTRACT

The rapid increase of Methicillin-resistant *Staphylococcus aureus* (MRSA) infections and the cross-resistance of MRSA to other antibiotics create an urgent demand for new therapeutic agents. Antimicrobial peptides (AMPs) are one of the most promising options for next-generation antibiotics. In this study, novel peptides were designed based on antimicrobial peptide fragments derived from *Aristicluthys nobilia* interferon-I to promote anti-MRSA activity and decrease adverse effects. Design strategies included substitutions of charged or hydrophobic amino acid residues for noncharged polar residues to promote amphipathicity. Two designed peptides, P5 (YIRKIRRFFKKLKKILKK-NH2) and P9 (SYERKINRHFKTLKKNLKKK-NH2), showed potent antimicrobial activities against both sensitive *Staphylococcus aureus* clinical isolates and MRSA strains without significant hemolysis or cytotoxicity to human hemocytes and renal epithelial cells. Scanning Electronic Microscopy (SEM) and qRT-PCR were employed to investigate the effects of P5 and P9 on *S. aureus* biofilm formation, morphology, and virulence-related gene expression. P5 and P9 significantly inhibited the biofilm and destroyed the cell membrane integrity, in addition to down-regulating several virulence factor genes and biofilm formation-related genes including *spa*, *hld*, and *sdrC*. P5 and P9 could be promising candidate antibacterial agents for the treatment of MRSA infections.

1. Introduction

With the abuse of antibiotics, a rising emergence of drug-resistant bacteria is occurring worldwide, threatening the efficacy and availability of antibiotics [1,2]. Methicillin-resistant *Staphylococcus aureus* (MRSA), one of the most common infection-resistant pathogens at present, can extend from skin infections to blood infections, posing a life-threatening risk to the patient or the injured. MRSA was first isolated in the UK in 1961 and has since become prevalent around the world [3]. In the 1980s, with the widespread use of third-generation cephalosporins in the clinic, the number of isolated MRSAs increased gradually. To this day, the detection rate of MRSA remains high. Due to parallel gene transfer, gene mutations and antibiotic screening, MRSA have acquired a variety of genes such as *mecA*, *spa*, *hld*, *sdrC*, and *hld* associated with antibiotic resistance [4]. Most MRSAs are also found to be resistant to non-β-lactam antibiotics, such as lincosamides, macrolides, aminoglycosides, quinolones and even multiple antibiotic combinations [5]. Unfortunately, with increased infections caused by MRSA, the effect of antibiotic treatment has become less optimistic [6]. Hence, there is an urgent need for new types of antibiotics,

* Corresponding author.
** Corresponding author.
*** Corresponding author. Key Biosensor Laboratory of Shandong Province, Biology Institute, Qilu University of Technology (Shandong Academy of Sciences), Jinan, 250103, China.
E-mail addresses: tyrm@jnu.edu.cn (R. Yu), xiaxk@sdas.org (X. Xia), lxzhang@ecust.edu.cn (L. Zhang).
[1] Chunlei Li and Chengguang Zhu made equal contribution to this work.

https://doi.org/10.1016/j.ejmech.2019.111686
0223-5234/

especially for treating drug-resistant *S. aureus* pathogens.

Antimicrobial peptides (AMPs) are also called host defence peptides. They are generated by the host organism as a result of the innate immune defence found in all classes of life [7,8]. Due to the increasing number of antibiotic resistance problems, there is currently a lot of interest in new treatments, including AMPs. Because of their modes of action, lack of bacterial resistance, and lack of adverse effects in humans, AMPs are now considered dependable alternative treatments in the development of novel antibacterial therapies. So far, several AMPs has been approved for marketing, such as Daptomycin, Bacitracin, Polimyxin B, Colistin, Tyrothricin and Gramicidin, and at least 20 AMPs are in the process of application or clinical research [9–11]. AMPs are usually short cationic peptides with 10–50 amino acid residues with a common physicochemical characteristic of abundant hydrophobic and positively charged amino acids to form an amphipathic structure. The amphipathic structure of AMPs triggers their adsorption at the bacterial membrane surface, which consists of negatively charged lipids, allowing their translocation across the cytoplasmic membrane. This translocation may trigger either membrane permeabilization, interfering with membrane-associated enzymes involved in bacterial cell wall synthesis, or attack on intracellular targets, eventually causing cell death [12–14]. Although AMPs' unique mechanism of action renders it a new generation of antibacterial drugs to replace traditional antibiotics, potential cytotoxicity and hemolysis hinder its further research and development [9,15]. Recently, several AMPs were designed based on natural peptides such as LL-37, Cathelicidin BF and Magainin 2 which showed high bacteria selectivity and clinical potential [16–18]. Therefore, designing novel antimicrobial peptides is one approach to improving the biological activity of AMPs and overcoming existing deficiencies.

Interferons (IFNs) are essential cytokines possessing multifunction in innate and adaptive immunity widely distributed amongst vertebrates [19]. IFNs are divided into three types, namely IFN-I (mainly IFN-α/β), IFN-II (IFN-γ), and IFN-III (IFN-λ), based on their differences in gene structure and cellular function [20]. As clearly reported, IFN-I promoted the release of nitric oxide and pro-inflammatory cytokines through dendritic cells and macrophages, further enhancing the host's antimicrobial activity to defeat viral and microbial infections [21]. In last decade, IFN-I and IFN-II have been reported in some teleosts including zebrafish, pufferfish, Atlantic salmon, and bighead carp *Aristicluthys nobilia* [22–25], and IFN-I was demonstrated to be vital during bacterial infections [26], suggesting it is a significant host defense molecule. Interestingly, it was recently found that IFN-I was capable of directly exerting antimicrobial activity [27], whereas, the potential peptide fragments possessing activity in IFN-I were not fully revealed. Previously, we identified an AMP fragment from *A. nobilia* IFN-I which was the fifth helical motif of IFN-I named as H5, which showed moderate antimicrobial activity against several pathogens including *S. aureus* ATCC 25923, *Streptococcus mutans* ATCC UA159, and *Candida albicans* ATCC 5314. In this study, we designed a series of peptides (P1–P12) based on H5 to improve antibacterial activity. After screening antimicrobial activity, cytotoxicity and hemolytic activity, P5 and P9 exhibited excellent activity toward *S. aureus*, especially MRSA. As such, we envision that these peptides could yield potent antibiotics with minimal hemolysis and no apparent cytotoxicity to human hemocytes and renal epithelial cells, and thereby more promise of future development for practical use in therapeutics.

2. Results

2.1. Physicochemical characterization of peptides

Twelve peptides were designed to enhance amphipathicity of AMP H5, which could help the peptides penetrate the bacterial cell membrane and eventually lead to bactericidal action. H5-derived peptides with amino acid substitutions were synthesized using solid phase peptide synthesis (SPPS). Electrospray ionization mass spectrometry (ESI-MS) and high-performance liquid chromatography (HPLC) analysis were used to verify the fidelity of the synthesized peptides as presented in Table 1 and Supplementary Fig. S2. The observed molecular weight of the synthesized peptides showed no noticeable difference from the theoretical molecular weight, indicating successful synthesis of the peptides. Table 1 and Fig. 1 summarize the physicochemical characterization of peptides. All the peptides (ranging from 18 to 20 amino acid residues) possessed highly positive-net charges. H5 exhibited a +6-net charge which was the lowest positive charge among the designed peptides; furthermore, P6, P11, and P12 displayed a +11-net charge. Except for the greater hydrophilic character of P8 and P9, the ratios of polar residues to nonpolar residues of the remaining peptides were about 60%. Correspondingly, P8 and P9 showed lower hydrophobicities, 0.016 and −0.125, respectively, and P4 had the highest hydrophobicity of 0.326. However, the highest hydrophobic instance among the peptides was P5. Fig. 1 shows the predicted helical wheel diagrams of the peptides. All the peptides could form helixes, and further possessed an amphipathic structure forming a hydrophilic and hydrophobic side.

Note: Lys (K) and Arg (R) were assigned with +1 charge. Asp (D) and Glu (E) were assigned with −1 charge. L: length (aa); pI: isoelectric point; T. Mw: theoretical molecular weight; O. Mw: observed molecular weight; NC: net charge; H: hydrophobicity; HM: hydrophobic moment; PR: polar residues; NPR: nonpolar

Table 1
Physicochemical properties of the designed peptides.

Peptide	Sequence	L	pI	T. Mw	O. Mw	NC	H	HM	PR/n%	NPR/n%
H5	YEIKINRHFKTLKKNLKK-NH2	18	10.39	2301.81	2300.8	+6	0.075	0.499	12/66.67	6/33.33
P1	YIRKINRHFKTLKKNLKK-NH2	18	11.30	2328.88	2327.9	+8	0.054	0.715	12/66.67	6/33.33
P2	YIRKIRRFFKTLNKNLKK-NH2	18	11.76	2366.93	2365.9	+8	0.146	0.768	11/61.11	7/38.89
P3	YIRKIRRFFKKLNKNLKK-NH2	18	11.77	2394.00	2393.0	+9	0.076	0.802	11/61.11	7/38.89
P4	YFRTIRRFFKKLFKTLKK-NH2	18	11.76	2421.02	2420.6	+8	0.326	0.822	10/55.56	8/44.44
P5	YIRKIRRFFKKLKKILKK-NH2	18	11.78	2407.10	2406.8	+10	0.188	0.830	10/55.56	8/44.44
P6	YIRKIRRFFKKRFKFRKK-NH2	18	12.19	2546.20	2545.2	+11	0.041	0.566	11/61.11	7/38.89
P7	WVRKVRRWWKKVKKVVKK-NH2	18	12.32	2438.08	2438.0	+10	0.161	0.822	10/55.56	8/44.44
P8	SYEIKINRHFKTLKKNLKKK-NH2	20	10.47	2517.06	2517.2	+7	0.016	0.413	14/70.00	6/30.00
P9	SYERKINRHFKTLKKNLKKK-NH2	20	10.79	2560.09	2560.0	+8	−0.125	0.545	15/75.00	5/25.00
P10	WYERLINRKFKWLKGRLSKK-NH2	20	11.79	2794.56	2794.8	+7	0.254	0.533	12/60.00	8/40.00
P11	LYKRYILRKFKFLKKKLKKK-NH2	20	10.93	2670.46	2670.4	+11	0.158	0.371	11/55.00	9/45.00
P12	VWKRWVVRKWKWVKKKVKKK-NH2	20	12.07	2724.47	2724.0	+11	0.208	0.407	11/55.00	9/45.00

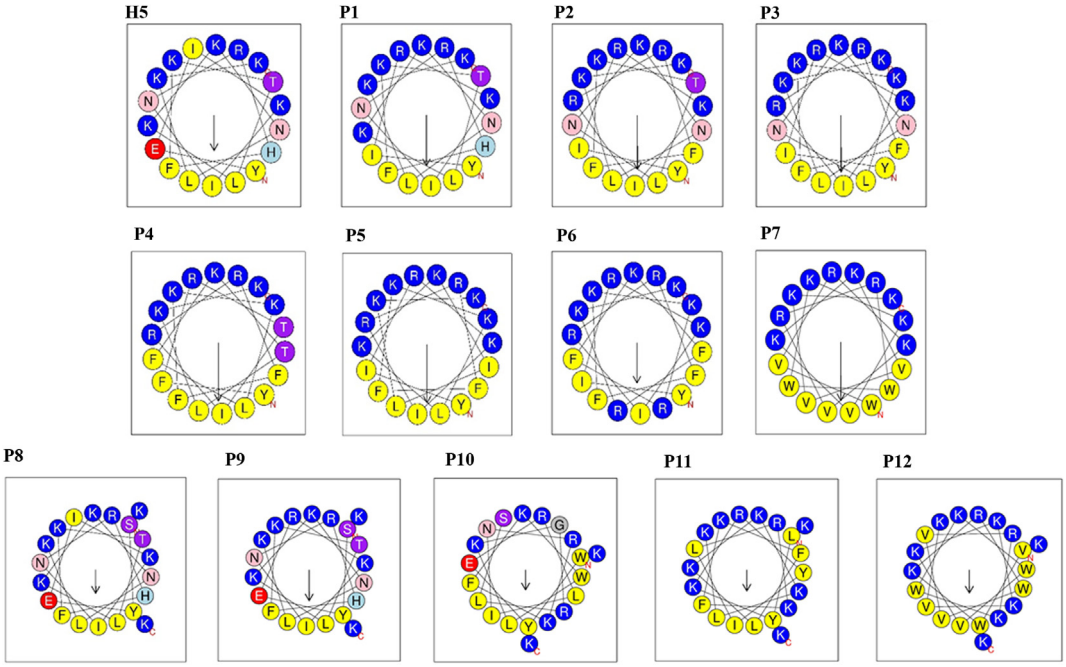

Fig. 1. Designed peptides with antimicrobial activities possess an amphipathic helix structure. The hydrophobic residues are yellow, positively charged hydrophilic residues are blue, and negatively changed hydrophilic residues are red. The noncharged polar residues are purple. (For interpretation of the references to colour in this figure legend, the reader is referred to the Web version of this article.)

residues; The changed amino acids in each peptide compared with H5 were underlined.

2.2. Secondary structures of peptides

The secondary structures of peptides in aqueous and mimic hydrophobic membrane environments were determined using CD spectroscopy as shown in Fig. 2. All the peptides failed to form an α-helical conformation in 10 mM PBS except P2. In membrane-mimetic environments, the CD spectra of the peptides involving leucine and isoleucine, such as P5, showed two negative peaks at about 222 and 208 nm and demonstrated typical helical structure predisposition, while phenylalanine-rich peptides like P4 exhibited a unique α-helical conformation signal feature (Fig. 2). The close interactions between bi/multi-tryptophan, P7, P10, and P12, tryptophan-involving peptides, demonstrated a greater tendency to form a β-turn rather than an α-helical conformation in membrane-mimetic environments.

2.3. P5 and P9 inhibited the growth of MRSA

The antimicrobial activities of the peptides against *S. aureus* ATCC 25923, clinical MRSA strain 18466, *Streptococcus mutans* ATCC UA159, *S. sanguis* ATCC 10556, and *Candida albicans* ATCC 5314 was examined (Table 2). Among these peptides, P5 exhibited the highest antimicrobial activity against fungal pathogen *C. albicans*, gram-positive bacteria *S. aureus,* and *S. mutans* with the MIC of 32, 8 and 64 μg/mL, respectively. Notably, P5 exhibited good selectivity with a MIC as low as 8 μg/mL towards MRSA with (3 μM), compared to 64 μg/mL for the beneficial bacterium *S. sanguis* as it can inhibit the growth of *S. mutans* to prevent dental caries [28]. With a MIC of 16 μg/mL, P9 showed good inhibition of MRSA as well, but was two-fold weaker than P5, yet exhibited a similar selective effect towards *S. sanguis*. Our optimized native peptides, P5 and P9 were at least eight and four times more inhibitory towards *S. aureus*, respectively, compared to H5. Furthermore, P2, P4, P6, P9, and P11 also showed moderate broad-spectrum antimicrobial activity. P6 showed good inhibitory activity to all microorganisms in the experiment. The MIC of P6 towards *C. albicans*, *S. aureus*, *S. mutans*, MRSA and *S. sangui* were 32, 64, 16, 32, and 64 μg/mL, respectively, which demonstrates lower selectivity against pathogens and beneficial bacteria compared to P5 and P9.

The anti-*S. aureus*/MRSA activity of P5 and P9 against sixteen clinically isolated antibiotic-resistant *S. aureus* strains was tested, and the result showed MRSA was highly resistant to oxacillin and methicillin with the MIC over 1200 μg/mL (Fig. 3 and Supplementary Table S1). P5 exhibited broad-spectrum activity against these *S. aureus* strains, especially antibiotic-resistant strains, with MICs from 8 to 16 μg/mL, while Methicillin-Sensitive *S. aureus* (MSSA) ranged from 16 to 32 μg/mL (Fig. 3), indicating better inhibition of antibiotic-resistant strains. P9 showed similar activity against these *S. aureus* strains with MICs of 16–32 μg/mL. However, methicillin and oxacillin, clinical drugs administered for *S. aureus* infection, only inhibit four MSSA strains, ATCC 25923, 29213, 8325.4, and 6538, while showed no inhibitory activities against all of the MRSA strain (Supplementary Table S1).

2.4. P5 and P9 inhibited S. aureus without detectable resistance

We then measured whether the non-resistant *S. aureus* strains can acquire resistance to these two peptides (P5 and P9). Methicillin and oxacillin were served as the control. Serial passage of the two non-resistant *S. aureus* strains in the presence of sub-MIC levels of P5 and P9 over a period of 15 days failed to produce resistant mutants (Fig. 4) as P5 and P9 still inhibited the growth of *S. aureus* at same MIC level. However, the MICs of methicillin and oxacillin increased 8–16 times and 8 times, respectively (Fig. 4). The MICs of methicillin and oxacillin started to be elevated just after 2–5 days even though they did not possess the known resistant gene *mecA* (Fig. S1), indicating the fast resistance acquisition of drug sensitive *S. aureus* strains to methicillin and oxacillin (Fig. 4).

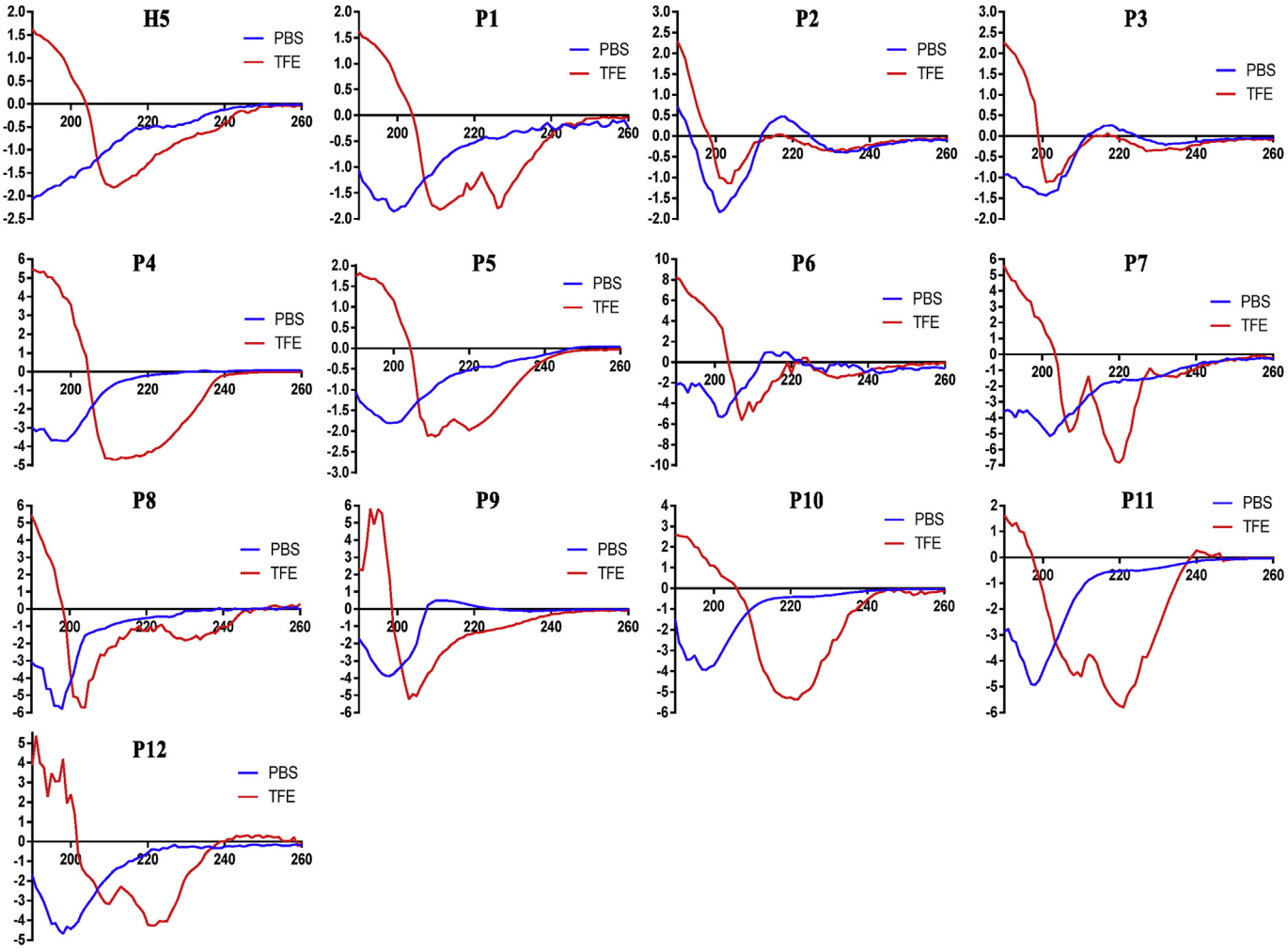

Fig. 2. Secondary structures of the designed peptides determined by circular dichroism spectroscopy.

Table 2
Antibacterial activity of the designed peptides.

Sample	MIC (μg/mL)				
	C. albicans ATCC 5314	*S. aureus* ATCC 25923	MRSA 18466	*S. mutans* ATCC UA159	*S. sangui* ATCC 10556
H5	<64	<64	<64	<64	<64
P1	<64	<64	<64	<64	<64
P2	<64	<64	<64	32	<64
P3	<64	<64	<64	<64	<64
P4	64	64	64	<64	<64
P5	32	8	8	64	<64
P6	32	64	32	16	64
P7	<64	<64	<64	<64	<64
P8	<64	<64	<64	<64	<64
P9	64	32	16	<64	<64
P10	<64	<64	<64	<64	<64
P11	<64	<64	64	<64	<64
P12	64	<64	<64	<64	<64
Vancomycin	–	1	1	2	1
Econazole	4	–	–	–	–

2.5. P5/P9 inhibited the biofilm formation and damaged the cell membrane of S. aureus

To investigate whether P5 and P9 can inhibit *S. aureus* biofilm formation, we subsequently randomly selected four strains, including two MSSA strains ATCC 29213 and 25923 and two MRSA strains 19498 and 18466. The SEM results showed that both P5 and P9 inhibited MSSA and MRSA biofilm formation (Fig. 5). There was an apparent decrease in the number of bacterial cells after P5 and P9 treatment, respectively. Notably, P9 significantly inhibited

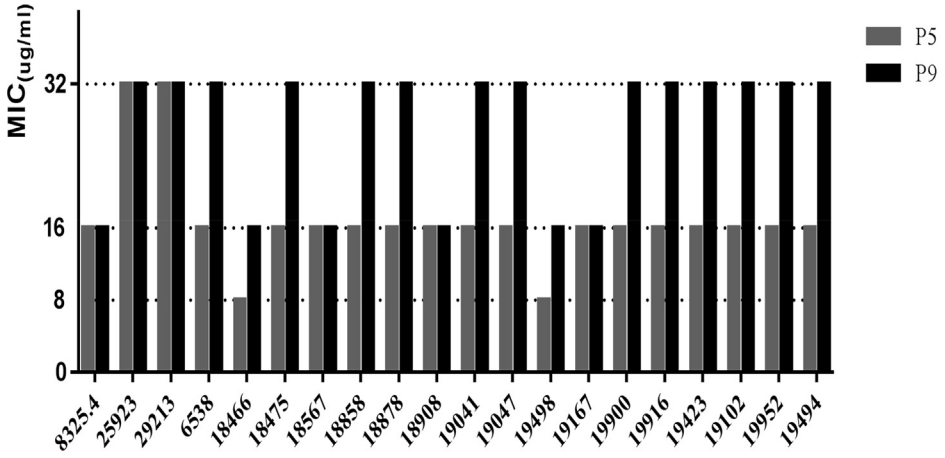

Fig. 3. Antibacterial activities of P5/9 against various Methicillin-sensitive *S. aureus* (MSSA) and Methicillin-resistant *S. aureus* (MRSA).

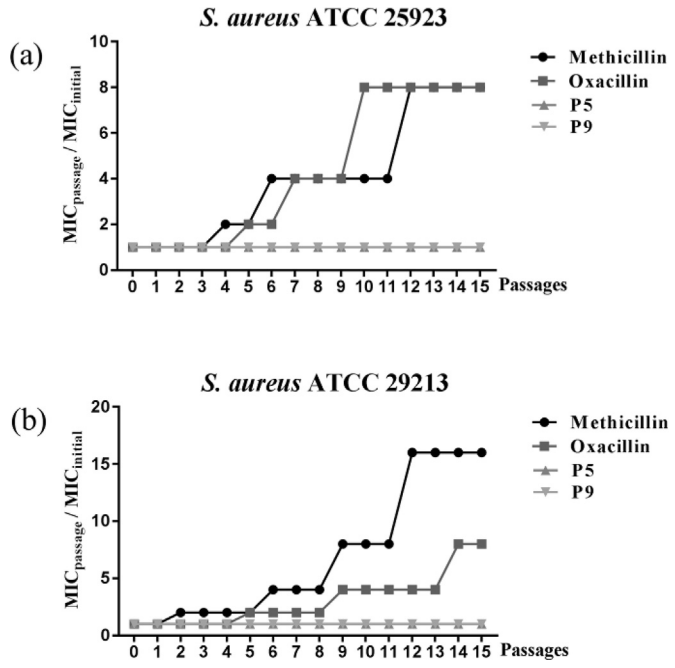

Fig. 4. Relative MIC ratio of each passages in contrast to the initial MIC revealed acquisition of drug resistance induced by methicillin, oxacillin, P5 and P9 against two *S. aureus* strains. (a) *S. aureus* 25923,(b) *S. aureus* 29213. MIC determinations were repeatedly performed from Passages 0 to 15 (Passages 0–15).

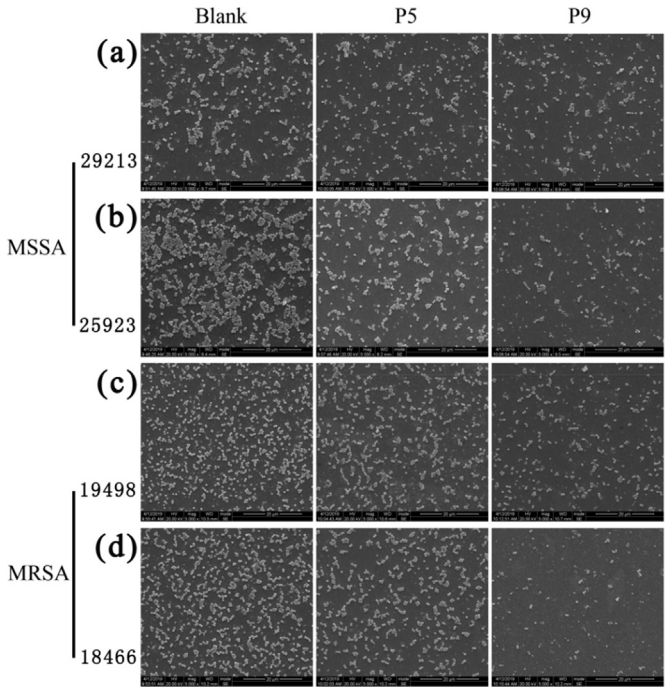

Fig. 5. SEM observation of biofilm formation of *S. aureus* ATCC 29213(a), ATCC 25923(b), MRSA 19498(c), MRSA 18466(d) affected by P5/P9. *S. aureus* with the vehicle group, P5 treated group and P9 MIC treated group.

biofilm formation particularly in the MRSA 18466 strain, as only a small number of bacterial cells remained, even better than that of MSSA.

There was a decrease in the number of bacteria as well as a significant change in the morphology of some cells. In the blank group, no morphological abnormalities had been found neither in MSSA 29213, 25923 strains nor MRSA 19498 and 18466 strains. After treatment with either P5 or P9, the MSSA and MRSA strains presented a decreased cell volume, cell membrane damage, and extravasation of cytoplasmic content (Fig. 6). The observed invagination (Fig. 6b,d), shrinking (Fig. 6a,b,c,d) and perforation (Fig. 6a) in the cell membrane indicated that P5/P9 destroyed the cell membrane integrity, further resulting in extravasation of cytoplasmic content and enlargement of the extracellular matrix (Fig. 6c). P9 showed better membrane disruption activity and decreased bacterial cell counts, particularly against the MRSA 18466 strain (Fig. 6d).

2.6. P5 and P9 reduced the virulent genes' expression of S. aureus

We evaluated the effects of P5 and P9 on MSSA and MRSA by measuring the expression of several biofilms or virulence-related genes, including *mecA*, *spa, hld, sdrC*. Among these genes, *mecA* was the only one that existed in MRSA, in line with its resistance to methicillin (Supplementary Fig. S1 and Table S1). The genes *spa* and *hld*, separately encoding *Staphylococcus* protein A and δ-lysin related to bacterial virulence [29,30], were significantly down-regulated in MRSA 19498 and 18466 while no detection in the MSSA group under the action of P5 or P9 (Fig. 7a and b). The gene *sdrC*, encoding adhesin and related to biofilm formation which can

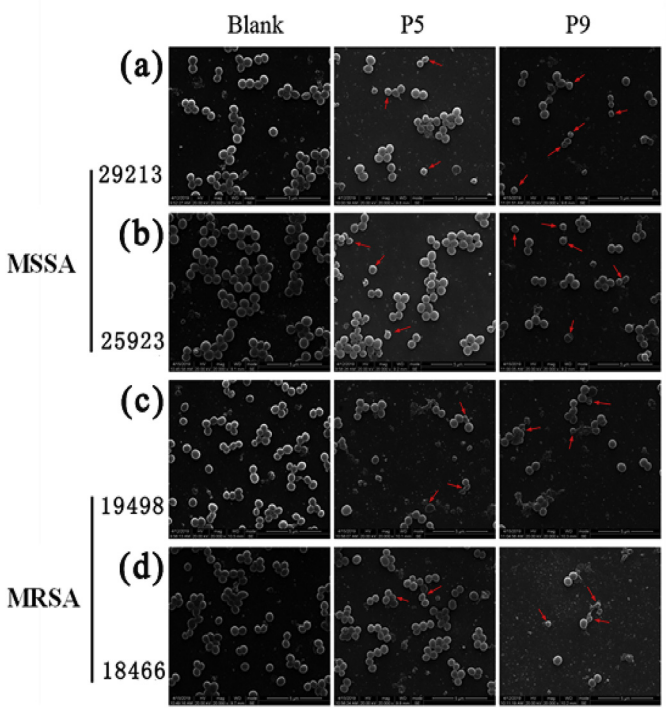

Fig. 6. SEM observation of biofilm formation of *S. aureus* ATCC 29213(a), ATCC 25923(b), MRSA 19498(c), MRSA 18466(d) with the control group and group treated with P5 or P9. Decrease of the bacteria and lysis of the cell membrane were observed after treatment; pointed out by the arrow.

promote bacteria proliferation on the skin and mucosa of the host [31], was also down-regulated in MRSA 19498 and 18466 treated with both these two peptides (Fig. 7c). The down-regulation of virulent genes indicates that P5 and P5 not only inhibit growth and MRSA biofilm formation but also reduce infectious virulence.

2.7. Hemolytic activity, stability and cytotoxicity

Hemolysis is a significant adverse effect of AMPs which hinders their application considerably. Hemolytic activity of all the AMPs are shown in Table 3. It was desirable that the Hmax of all AMPs was less than 35%. P8 was the optimal peptide which showed the lowest hemolytic activity with a Hmax of 6.78%. Representing poor peptide performance, P12 had the most robust hemolytic activity with a Hmax of 31.03% and induced 10% hemolysis at a concentration of 57.24 μg/mL. P7 and P10 also showed relatively powerful hemolytic activities, with a Hmax of 25.54% and 17.33%, respectively. However, both P5 and P9 showed high antimicrobial activity as well as low hemolytic effect (Supplementary Fig. S3), which induced less than 15% hemolytic effect even at the concentration of 640 μg/mL.

Note: HC_{10} and HC_{50} are the concentrations of peptide causing 10% and 50% hemolysis on murine erythrocytes, respectively. Hmax is the percentage (%) hemolysis at the highest peptide concentration tested (640 μg/mL).

To comprehensive evaluate the stability of the peptides P5 and P9, we determined their stability in blood plasma, bacterial supernatant and trypsin treatment, respectively. As demonstrated in Supplementary Fig. S4 and Fig. S5, P5 and P9 showed more stable in blood plasma and MRSA bacterial supernatant compared with trypsin treatment. One quarter concentration of P5 or P9 was found in blood plasma for 12 h incubation, and P5 or P9 were not found from 24 h blood plasma incubation (Figs. S4a and c). Inspiringly, these two peptides performed highly stability in MRSA bacterial

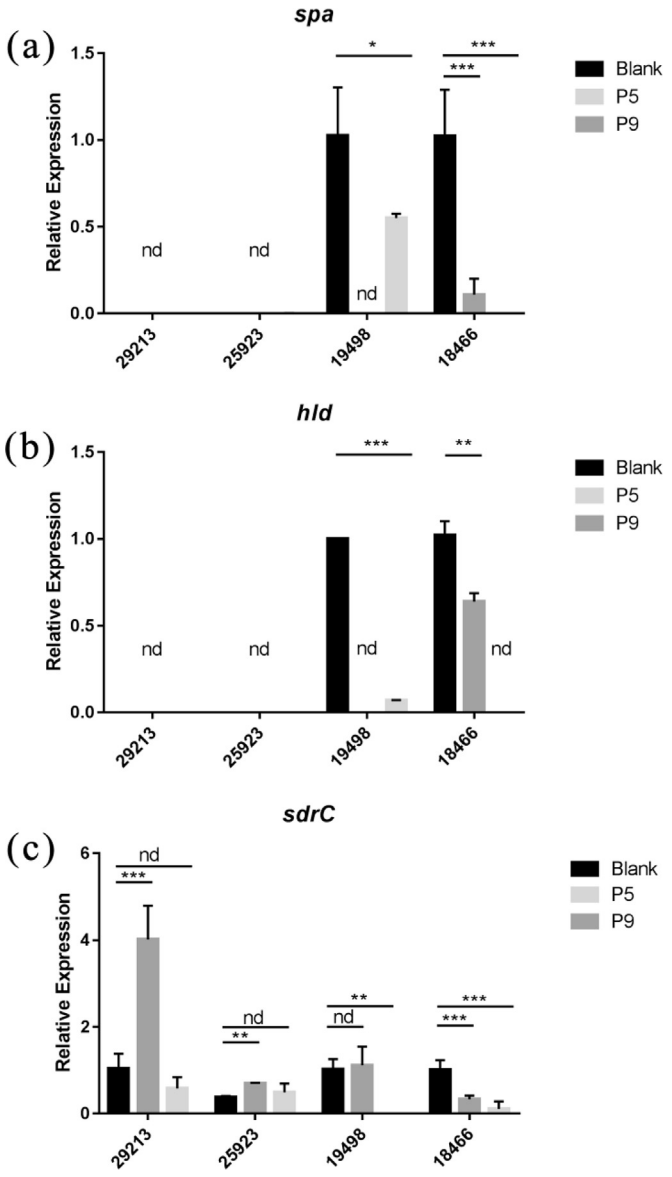

Fig. 7. Expression levels of the *spa*, *hld*, and *sdrC* genes determined by qRT-PCR in MSSA ATCC 29213 and 25923, MRSA clinical isolates 19498 and 18466 cultured in the presence or absence of MIC concentrations of P5/9. The densitometric results of the transcripts were quantified using 16s rRNA expression and analyzed by one-way ANOVA.

supernatant. There was a small amount of P5 or P9 obtained even after 24 h treatment with supernatants from MRSA (Figs. S4b and d). Among them, almost half of P5 concentration was not cleaved by bacterial supernatant for 12 h incubation, and nearly one-fifth of P5 concentration was detected in MRSA supernatant incubation for 24 h. Furthermore, the potential cytotoxicity of hydrolyzed metabolite peptides from P5 or P9 was assessed. As shown in Supplementary Fig. S6, the metabolites had no apparent cytotoxicity towards human embryonic kidney HEK293T cells. As is known, trypsin is one of the major proteolytic enzymes in the gastrointestinal tract [32,33], while trypsin degradation has less effect on AMP topical administration. Hence, P5 and P9 showed great potential via topical administration.

Numerous studies have shown that AMPs inhibit cell proliferation and trigger membrane disruption, thereby facilitating cell death [9]. Hence, the cytotoxicity assay against human embryonic

Table 3
Hemolytic activity of designed peptides.

Peptide	Hemolytic activity (μg/mL) ± SD		Percent hemolysis ±SD Hmax (100%)
	HC_{10}	HC_{50}	
H5	>640	>640	7.94 ± 2.1
P1	>640	>640	8.07 ± 2.5
P2	>640	>640	7.17 ± 3.4
P3	>640	>640	9.86 ± 4.2
P4	640	>640	10.30 ± 2.5
P5	640	>640	10.27 ± 2.2
P6	>640	>640	8.21 ± 1.2
P7	80.04 ± 7.2	>640	25.54 ± 6.2
P8	>640	>640	6.78 ± 2.4
P9	>640	>640	7.06 ± 3.7
P10	178.82 ± 12.6	>640	17.33 ± 6.8
P11	>640	>640	9.34 ± 3.8
P12	57.24 ± 5.2	>640	31.03 ± 9.3

kidney HEK293T cells was conducted using dose-response studies. As depicted in Fig. 8, the cell viabilities were approximately 70–80%, and no significant cytotoxicity against HEK293T cells was observed after treatment by most of the peptides at various concentrations from 5 to 640 μg/mL. Unfortunately, P7 and P12 eliminated approximately half of the living cells at a concentration of 640 μg/mL with cell viabilities of only 65.74% and 58.94%, respectively.

3. Discussion

Antimicrobial peptides (AMPs) are of increasing interest as potential potent antibiotics with simple structures. In the present study, a series of peptides with optimized properties were designed based on an antimicrobial peptide fragment H5 derived from IFN-I, among which P5 and P9 had the best antimicrobial activities, especially to MRSA. The vital rationale of AMPs shown in helical structures is amphiphilic, although the structure and sequence of AMPs are diverse [15]. It has been found that the amphipathic ordered structure, particularly the formation of α-helices, is associated with peptide-induced membrane disruption [34]; P5 and P9 happened to be perfect amphipathicity structures (Fig. 1). The amphiphilic structural properties as dispersed or complete segregation of hydrophobic and polar residues of AMPs are regarded to induce their folding to form the ideal three-dimensional conformation and exerting antimicrobial activity [35]. Several peptides like P6, P10, P11, and P12 showed imperfect amphipathicity and weak antimicrobial activity compared to P5 and P9 (Table 1). Besides the amphipathicity, hydrophobic amino acid residues like leucine, isoleucine, phenylalanine, and tryptophan were attributed to the enhanced antimicrobial activity of AMPs [36,37]. With the same amphipathicity structures as P5 and P9, the antimicrobial activities of P4 and P7 were lower than them because of the different amino acids located at their hydrophobic surfaces. The perfect hydrophobic surface forming with leucine and isoleucine but not phenylalanine and tryptophan was indicated to be beneficial to the antibacterial activity of H5. Our results suggest that not only the amphipathic structure of AMPs is important to antimicrobial activity, the types of hydrophobic amino acids in hydrophobic surfaces is also highly critical for bacterial killing.

The emergence and spread of bacterial resistance to antibiotic have become a serious challenge to global health [1–3]. We found that the sensitive *S. aureus* strains can easily acquire methicillin and oxacillin resistance (Fig. 4), even they did not harbour *mecA* gene (Fig. S1), indicating that sensitive *S. aureus* can easily develop new resistant mechanism against these clinical drugs. However, we were unable to obtain resistant mutants of *S. aureus* against P5 and P9 after serial passages over 15 days (Fig. 4), indicating the potential application of these two peptides against both resistant and sensitive strains.

Bacterial biofilms are formed by bacteria irreversibly binding to a surface and forming a matrix that is made up of extra-polymer substances. The formation of biofilm can facilitate the survival of bacteria by enhancing resistance to antibiotics and host immune defences [38–40]. They are hard to eradicate due to their more complex structure compared to planktonic bacterial cells. Interestingly, P5 and P9 were capable of deforming not only the biofilm but the cytoplasmic membrane of MSSA and MRSA strains as well, respectively. Treatment with MIC concentrations of P5/P9 resulted in a decrease in the number of MSSA and MRSA biofilm-forming microorganisms and inhibition of aggregation (Fig. 5). P5 and P9 both induced ruptured membranes and leakage of cellular components following treatment (Fig. 6).

Like many other AMPs, P5 and P9 might associate with the biofilm by means of binding to negatively charged constituents on the outer acidic surfaces, such as peptidoglycans and lipopolysaccharides, followed by membrane destabilization [41–43]. Furthermore, the biofilm disruption induced by P5/P9 might trigger biofilm or virulence-related genes, facilitating the bacteria cell death. Here we tested the expression levels of well-known virulence genes, *spa*, *hld*, and the vital regulatory gene *sdrC*, which is associated with adhesin encoding and biofilm formation for proliferation on the skin and mucosa of the host. Significant inhibition of *spa* and *hld* in MRSA occurred in the presence of either P5 or P9. (Fig. 7a and b). Interestingly, these two virulence genes were only expressed in MRSA strains, and no expression was detected in MRSA strains, indicating a heightened virulence of MRSA strains. Another biofilm-

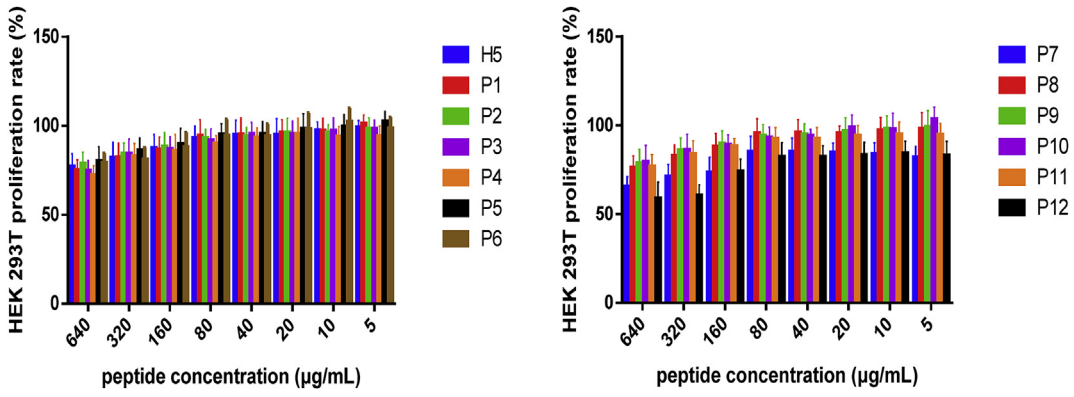

Fig. 8. Cytotoxicity of the designed peptides against HEK 293T cells.

related gene *sdrC* was also down-regulated in MRSA (Fig. 7c). P5 and P9 in our study represent dual-functional AMPs by not only inhibiting the growth and biofilm formation through the disruption of the bacterial cell membrane and permeabilization on the biofilms but also reducing the infectious virulence by inhibiting the expression virulence factors, especially in MRSA strains.

The key to the therapeutic application of AMPs is that it not only selectively and effectively destroys bacteria and other pathogens but causes minimal damage to human cell membranes [44]. The designed peptides showed no apparent cytotoxicity and low hemolytic effect except P7 and P12 (Table 3 & Fig. 8). Even the metabolite peptides of P5 or P9 produced by trypsin digestion showed no obvious cytotoxicity (Supplementary Fig. S5). Possessing an α-helical structure and adequate net positive charges, P5 and P9 showed higher selectivity when considering the antibacterial activity and cytotoxicity likely in part due to its great symmetric amphipathic property [45]. It has reported that the peptides with tryptophan residues which located adjacent to the cationic sector induced a powerful permeabilizing activity and showed high cytotoxicity [46].

P5 and P9 showed stability against blood plasma and bacterial supernatants but vulnerable to trypsin digestion (Supplementary Fig. S4 and Fig. S5). It indicated that P5 and P9 might exhibit antibacterial effect via topical administration in case it degrades in gastrointestinal tract. Furthermore, the trypsin metabolites of P5 and P9 showed no apparent cytotoxicity towards human normal kidney cells (Supplementary Fig. S6). Hence, P5 and P9 showed great potential to be used via topical administration. In conclusion, based on the antibacterial peptide H5, we designed two amphipathic peptides P5 and P9 with potent activity against various MRSA (MICs 8 μg/mL, 16 μg/mL, respectively) with a suspected membrane-disrupting mode of action. P5 and P9 were demonstrated to be bactericidal and non-toxic towards human hemocytes and renal epithelial cells and had the capability to influence the gene expressions of virulence factors. Therefore, P5 and P9 showed potential as promising antibacterial agents against MRSA. Moreover, these findings provided a reference for peptide rational design and optimization.

4. Experimental section

4.1. Materials and strain culture conditions

Sixteen Methicillin-resistance *S. aureus* (MRSA) clinical isolates were collected from the Beijing Chaoyang Hospital, then conducted the drug sensitivity of both oxacillin and methicillin (Supplementary Table S1). Four methicillin-sensitive *S. aureus* reference strains were also employed, including *S. aureus* ATCC 25923, *S. aureus* ATCC 29213, *S. aureus* ATCC 8325.4 and *S. aureus* ATCC 6538. Other fungus and bacteria served as antimicrobial controls, including *C. albicans* ATCC 5314, *S. mutans* ATCC UA159 and *S. sanguis* ATCC 10556. *S. aureus* strains were aerobically cultured in tryptic soy broth (TSB) at 37 °C for 18–24 h with vigorous shaking. Growth inhibition tests were performed according to CLSI guidelines in Mueller-Hinton broth (MHB). *S. mutans* and *S. sanguis*, which were cultured and tested in the Brain Heart Infusion Medium (BHI), were incubated aerobically at 37 °C with 5% CO_2 without shaking. *C. albicans* was grown in Yeast Extract Peptone Dextrose Medium (YPD) or RPMI 1640 Medium to perform anti-fungal susceptibility testing. All strains were stored at −80 °C until used.

4.2. Peptide design and synthesis

The peptide fragment possessing antimicrobial activity in IFN-I was the fifth helix motif designated as H5. Twelve peptides (P1~P12) were designed based on the antimicrobial fragment of interferon-I of bighead carp, H5. Design strategies included substitutions of charged or hydrophobic amino acid residues for non-charged polar residues to promote amphipathicity. Glu2 and Ile3 of H5 (YEIKINRHFKTLKKNLKK) was substituted with Ile2 and Arg3 to generate P1 (YIRKINRHFKTLKKNLKK), Glu2, Ile3, Asn6, and His8 of P1 were substituted by Ile2, Arg3, Arg6 and Phe8 to generate P2 (YIRKIRRFFKTLNKNLKK), Glu2, Ile3, Asn6, His8 and Thr11 of H5 were substituted with Ile2, Arg3, Arg6, Phe8 and Lys11 to generate P3 (YIRKIRRFFKKLNKNLKK), Glu2, Ile3, Lys4, Asn6, His8, Thr11, Lys13 and Asn15 of H5 were substituted with Ile2, Arg3, Thr4, Arg6, Phe8, Lys11, Phe13 and Thr15, to generate P4 (YFRTIRRFFKKLFKTLKK), Asn15 of P3 was substituted with Ile15 to generate P5 (YIRKIRRFFKKLKKILKK), Thr11, Leu12, Lys13, Asn15 and Leu16 of P3 was substituted with Lys11, Arg12, Phe13, Phe15 and Arg16 to generate P6 (YIRKIRRFFKKRFKFRKK), Tyr1, Glu2, Ile3, Ile5, Asn6, His8, Phe9, Thr11, Leu12, Asn15 and Leu16 of H5 were substituted with Trp1, Val2, Arg3, Val5, Arg6, Trp8, Trp9, Lys11, Val12, Val15 and Val16 to generate P7 (WVRKVRRWWKKVKKVVKK), a Ser1 and a Lys20 were inserted before Tyr1 after Lys18 of H5 to generate P8 (SYEIKINRHFKTLKKNLKKK), Ile4 of P8 was substituted by Arg4 to generate P9 (SYERKINRHFKTLKKNLKKK), Ser1, Lyr5, His9, Thr12, Lyr15, Asp16, and Lyr18 of P9 were substituted with Trp1, Leu5, Arg9, Trp12, Gly15, Lyr16, and Ser18 to generate P10 (WYERLINRKFKWLKGRLSKK), Ser1, Glu3, Lys5, Asn7, His9, Thr12 and Asn16 of P9 were substituted by Leu1, Lys3, Tyr5, Leu7, Lys9, Phe12 and Lys16 to generate P11 (LYKRYILRKFKFLKKKLKKK), Leu1, Tyr2, Tyr5, Ile6, Leu7, Phe10, Phe12, Leu13 and Leu17 of P11 were substituted by Val1, Trp2, Trp5, Val6, Val7, Trp10, Trp12, Val13 and Val17 to generate P12 (VWKRWVVRKWKWVKKKVKKK). C-termini of all the peptides were amidated (-NH2).

All the designed peptides were synthesized using solid phase peptide synthesis (SPPS) with CS336X automatic peptide synthesizer (CSBio. Ltd., US). When the synthesis was finished, the Fmoc group at the N-terminal was deprotected first, afterward; the side chain protection group was deprotected, and the peptide cleaved off from the Resin. The peptides were purified via reversed-phase high-performance liquid chromatography (RP-HPLC) and further analyzed by RP-HPLC and mass spectrometry to confirm their purity as greater than 95% (Supplementary Fig. S2).

4.3. Physicochemical characterization and secondary structure analysis

The physicochemical parameters of the designed peptides were analyzed using the ExPASy Bioinformatics Resource Portal (http://www.expasy.org/tools/), and the helix structure of the designed peptides was calculated by HeliQuest (http://heliquest.ipmc.cnrs.fr/). The secondary structure of designed peptides in different microbial membrane conditions was determined. Solutions of 10 mM PBS and 50% trifluoroethanol (TFE) mimicked aqueous and hydrophobic environments, respectively [17]. Triplicate spectra were recorded using a circular dichroism (CD) spectrometer (Chirascan, Applied Photophysics Ltd, UK) with a scanning wavelength range from 195 to 250 nm and a speed of 10 nm/min. The final sample concentration was 150 μM.

4.4. Determination of the antibacterial spectrum and minimum inhibitory concentration

Antibacterial activities of the peptide were determined against *S. aureus* ATCC 25923, *S. aureus* ATCC 29213, *S. aureus* ATCC 8325.4, *S. aureus* ATCC 6538, *S. mutans* ATCC UA159 and *S. sanguis* ATCC 10556. Clinically isolated *S. aureus* 18466, 18475, 18567, 18858,

18878, 18908, 19041, 19047, 19498, 19167, 19900, 19916, 19423, 19102,19952, 19494 was provided by Beijing Chaoyang Hospital and followed by drug sensitivity tests of oxacillin and methicillin. MIC of the peptides, oxacillin, methicillin and vancomycin susceptibility measurements were conducted in flat bottom, 96-well microtiter plates (Greiner, Germany), in accordance with a broth microdilution protocol modified from the Clinical and Laboratory Standards Institute M07-A9 methods (National Committee for Clinical Laboratory Standards 2012). The *S. aureus* were inoculated and grown to mid-log phase in fresh tryptic soy broth (TSB) at 37 °C, while *S. mutans* and *S. sanguis* cultivated in Brain Heart Infusion Medium (BHI) at 37 °C with 5% CO_2. Bacterial inoculum suspensions were adjusted the diluted to a final concentration of $0.5-2.5 \times 10^5$ CFU/mL in Mueller-Hinton broth (MHB). Peptides, oxacillin and methicillin were 2-fold serially diluted to make different concentrations from 0.5 to 64 μg/mL. Vancomycin was prepared in the same method with concentrations ranged from 0.125 to 16 μg/ml 100 μl of inoculum suspensions were then added to each well of the sterile 96-well plate with different concentrations of peptides, and the plate was incubated for 24 h at 37 °C. Broth with vancomycin or without bacteria was performed as the positive control or the negative control. MIC was considered as the lowest concentration of compounds that prevented visible turbidity by visual inspection. All experiments were done in triplicate.

The antifungal activities were performed in RPMI-1640 medium by broth microdilution assay according to the Clinical and Laboratory Standards Institute (CLSI) M27. The *C. albicans* ATCC 5314 were cultured in Yeast Extract Peptone Dextrose Medium (YPD) at 35 °C overnight. Then suspensions were adjusted at a final concentration of approximately $0.5-2.5 \times 10^4$ CFU/mL in RPMI-1640 medium. Peptides or econazole were 2-fold serially diluted to make different concentrations from 0.5 to 64 μg/mL or 0.125–8 μg/mL, respectively. A total of 100 μl cell suspension was added to a sterile flat bottom, 96-well microtiter plates with ranges concentrations of compound described above. Pure broth alone or with econazole was used as the negative control or the positive control, respectively. The plate was incubated at 35 °C for 24 h. MIC was considered the lowest concentration at which no fungal growth was visually observed under experimental conditions. Experiments were performed in triplicate with three biological replicates.

4.5. Drug resistance assays against antibacterial agents

To further determine whether *S. aureus* could develop resistance against antibiotics and AMPs, MIC measurements following repeated serial passages were performed as a previous method [47]. The MIC of methicillin, oxacillin, P5 and P9 against *S. aureus* ATCC 25923, *S. aureus* ATCC 29213 were measured as previous described in Section 4.4. A total 100 μl of the *S. aureus* suspensions in the sub-MIC well, in which agents and AMP concentrations were half-MIC and visible bacteria growth could be found, was taken and inoculated into 5 mL of fresh tryptic soy broth (TSB) at 37 °C. The overnight bacterial suspensions were diluted to approximately $0.5-2.5 \times 10^5$ CFU/mL in Mueller-Hinton broth (MHB) for the next MIC test. All of the MIC tests were repeatedly performed for 15 passages. The relative ratio of the MIC of each passage in contrast to the initial MIC was calculated. Repeated exposures to methicillin, oxacillin, P5 or P9, the increasing in relative ratio of the MIC would indicate the acquisition of drug resistance by *S. aureus*. The tests were performed in triplicate with three biological replicates.

4.6. Hemolytic assays

Murine blood was treated with citric acid to prevent clotting and then centrifuged at 3000×*g* for 5 min to obtain the erythrocytes. After washed thrice with 0.9% saline solution, the erythrocytes resuspended to 10 mM PBS (pH 7.4) were further treated with serial dilutions of the designed peptides using a 96-well plate for 1-h. A 10 mM PBS (pH 7.4) solution and 1% Triton X-100 treatment were used for 0 and 100% hemolysis, respectively. Hemolysis was expressed as the hemoglobin content obtained from the absorbance of the supernatant at 570 nm after centrifugation [48]. HC_{10} and HC_{50} are the concentrations of peptide causing 10% and 50% hemolysis on murine erythrocytes, respectively. Hmax is the percentage (%) hemolysis at the highest peptide concentration tested (640 μg/mL). This experiment was performed thrice.

4.7. Cell viability assays

The cell density of human HEK293T embryonic kidney cells was adjusted (1×10^5 cells/mL) and incubated using Dulbecco's modified Eagle's medium (DMEM) including streptomycin (100 μg/mL), penicillin (100 U/mL), and 10% fetal calf serum at 37 °C with 5% CO_2 environment. The designed peptides and the metabolite peptides of P5 or P9 that treated with trypsin for 4 h with various concentrations ranging from 5 to 640 μg/mL were added in the 96-well plates and incubated for 48 h at 37 °C. Cell viability was examined by 3-(4,5-Dimethylthiazol-2-yl)-2,5-diphenyltetrazolium bromide (MTT) reduction assays [48]. The resulting solution was determined at OD_{570} with a microplate reader (Synergy 2, Biotech, VT, USA). This assay was conducted in triplicate.

4.8. Examination the effect of bacterial biofilm formation and bacterial membrane damage by SEM

Overnight cultures of *S. aureus* and MRSA were diluted to approx. 10^8 CFU/mL for biofilm formation in Tryptic Soy Broth Medium (TSB). 1 mL of the suspension was added to the 12-well plate with the presence or absence of MIC concentrations of P5/9. After setting a sterile slice in each well, the plate was cultured for 24 h at 37 °C. The specimen was immersed in 2.5% glutaraldehyde in PBS for 4-h to overnight in a 4 °C refrigerator. Following a three-time rinse with PBS, the specimen was dehydrated using successive 5–15 min treatments, with 30%, 50%, 70%, 80%, 85%, 90%, 95%, and 100% ethanol. The specimen was rinsed with 100% hexamethyldisilazane and set on a piece of filter paper in a partially covered glass Petri and let dry overnight, then imaged on SEM at a range of magnifications.

4.9. Quantification of gene expression with qRT-PCR

S. aureus and MRSA isolates grown overnight were adjusted to 10^8 CFU/mL, then incubated in MHB with or without MIC concentrations of P5/9 for 1-h. RNAs were extracted from 5 mL cultures. Bacterial cultures were harvested by centrifugation at 12,000×*g* for 2 min at 4 °C. Pellets were rinsed with 1 mL TRIzol and lysed with 0.5 mL of zirconia-silica beads (diameter, 0.1 mm) in a high-speed homogenizer. RNA was isolated with DNA/RNA Extraction Reagent (Chloroform:Isoamylol = 24:1, Solarbio), High-Salt Solution for Precipitation (Plant, Takara), isopropanol, and 70% ethyl alcohol, which eventually dissolved in diethyl pyrocarbonate (DEPC) water.

cDNAs synthesized by PrimeScript™ RT reagent Kit with gDNA Eraser (Perfect Real Time, Takara) after genomic DNA in the solution containing RNA was degraded, according to the manufacturer's instructions. Quantitative reverse transcription-PCR (qRT-PCR) was carried out using the LightCycler 480 II System (Forrenstrasse 2,6343 Rotkreuz, Switzerland) and TB Green™ Premix Ex Taq™ II (Tli RNaseH Plus, Takara) according to the manufacturer's instructions. The expression level of 16S rRNA was used to normalize

that of other genes, which is widely used as an internal control. All experiments were repeated at least three times, and the primer sequences used in this study are publically available (Supplementary Table S2).

4.10. Stability of P5 and P9

The peptides, P5 or P9 with concentration of 20 μM were subjected to incubation in murine blood plasma or in the supernatant of MRSA growth at 37 °C. At the appropriate time points (0 h, 12 h and 24 h), the mixtures were analyzed via HPLC.

The trypsin hydrolysis was carried out in PBS solution using a 1:20 (w/w) enzyme to substrate ratio. P5 or P9 with 20 μM peptide concentration was mixed with enzyme solution and further incubated at 37 °C with agitation. At the appropriate time points (0 h, 0.5 h, 1 h, 2 h and 4 h), the mixtures were analyzed via HPLC.

Analysis of peptides and degradation products was performed using reversed-phase chromatography. The stationary phase was a 4.6 mm × 250 mm Excel AQ C-18 column from ACE (Aberdeen, Scotland). The mobile phase was composed of a gradient of distilled water (+0.1% trifluoroacetic acid) and acetonitrile (+0.1% trifluoroacetic acid) from 5% to 100% for 35 min with a flow rate of 1 mL/min, and detected at 220 nm.

4.11. Statistical analysis

Statistical analysis was performed by GraphPad Prism 6.0 (GraphPad Software, CA, USA). The experimental data are presented as the mean ± standard deviation (SD) unless otherwise indicated.

Conflicts of interest

The authors declare no conflict of interest.

Acknowledgement

We gratefully acknowledge the financial support of National Natural Science Foundation of China (No. 31770024, 81600858, 81870778, 31720103901, 31430002), National Key R&D Program of China (No. 2017YFF0209900), Ocean and Fisheries Science and Technology Development Projects of Guangdong (No. A201501C04), Major Science and Technology Projects/Significant New Drugs Creation of Guangdong (No. 2013A022100032), Natural Science Foundation from Shandong Province (No. ZR2017MH025, ZR2017ZB0206), and Taishan Scholars Program of Shandong Province for Lixin Zhang, the Youth Fund of Shandong Academy of Sciences (2018QN0029).

Appendix A. Supplementary data

Supplementary data to this article can be found online at https://doi.org/10.1016/j.ejmech.2019.111686.

References

[1] N. Téné, E. Bonnafé, F. Berger, A. Rifflet, L. Guilhaudis, I. Ségalas-Milazzo, B. Pipy, A. Coste, J. Leprince, M. Treilhou, Biochemical and biophysical combined study of bicarinalin, an ant venom antimicrobial peptide, Peptides 79 (2016) 103–113.
[2] C.L. Ventola, The antibiotic resistance crisis, PT 40 (2015) 277–283.
[3] Y. Rhee, A. Aroutcheva, B. Hota, R.A. Weinstein, K.J. Popovich, Evolving epidemiology of *Staphylococcus aureus* bacteremia, Infect. Control Hosp. Epidemiol. 36 (2015) 1417–1422.
[4] H.F. Chanbers, F.R. Deleo, Waves of resistance: *Staphylococcus aureus* in antibiotic era, Nat. Rev. Microbiol. 79 (2009) 629–641.
[5] C.J. Chen, Y.C. Huang, New epidemiology of *Staphylococcus aureus* infection in Asia, Clin. Microbiol. Infect. 20 (2014) 605–623.
[6] S. Thangamani, H. Mohammad, M.F. Abushahba, T.J. Sobreira, V.E. Hedrick, L.N. Paul, M.N. Seleem, Antibacterial activity and mechanism of action of auranofin against multi-drug resistant bacterial pathogens, Sci. Rep-UK 6 (2016) 22571.
[7] M. Zasloff, Antimicrobial peptides of multicellular organisms, Nature 415 (2002) 389–395.
[8] K.A. Brogden, Antimicrobial peptides: pore formers or metabolic inhibitors in bacteria? Nat. Rev. Microbiol. 3 (2005) 238–250.
[9] K.E. Greber, M. Dawgul, Antimicrobial peptides under clinical trials, Curr. Top. Med. Chem. 17 (2016) 620–628.
[10] F. Costa, C. Teixeira, P. Gomes, M.C.L. Martins, Clinical application of AMPs, in: K. Matsuzaki (Ed.), Antimicrobial Peptides. Advances in Experimental Medicine and Biology, Springer, Singapore, 2019, pp. 281–298.
[11] Drugs@FDA, FDA Approved Drug Products, 2019 accessed, https://www.accessdata.fda.gov/scripts/cder/daf/index.cfm/. (Accessed 30 July 2019).
[12] C.D. Fjell, J.A. Hiss, R.E. Hancock, G. Schneider, Designing antimicrobial peptides: form follows function, Nat. Rev. Drug Discov. 11 (2011) 37–51.
[13] Y. Wang, Z. Zhang, L. Chen, H. Guang, Z. Li, H. Yang, J. Li, D. You, H. Yu, R. Lai, Cathelicidin-BF, A snake cathelicidin-derived antimicrobial peptide, could be an excellent therapeutic agent for acne vulgaris, PLoS One 6 (2011), e22120.
[14] W. Chen, B. Yang, H. Zhou, L. Sun, J. Dou, H. Qian, W. Huang, Y. Mei, J. Han, Structure-activity relationships of a snake cathelicidin-related peptide, BF-15, Peptides 32 (2011) 2497–2503.
[15] L. Zhang, R.L. Gallo, Antimicrobial peptides, Curr. Biol. 26 (2016) R1–R21.
[16] G. Wang, J.L. Narayana, B. Mishra, Y. Zhang, F. Wang, C. Wang, D. Zarena, T. Lushnikova, X. Wang, Design of antimicrobial peptides: progress made with Human Cathelicidin LL-37, Adv. Exp. Med. Biol. 1117 (2019) 215–240.
[17] L. Jin, X. Bai, N. Luan, H. Yao, Z. Zhang, W. Liu, Y. Chen, X. Yan, M. Rong, R. Lai, Q. Lu, A designed tryptophan- and lysine/arginine-rich antimicrobial peptide with therapeutic potential for clinical antibiotic-resistant *Candida albicans* vaginitis, J. Med. Chem. 59 (2016) 1791–1799.
[18] B. Pandey, S. Srivastava, M. Singh, J. Ghosh, Inducing toxicity by introducing a leucine-zipper-like motif in frog antimicrobial peptide, magainin 2, Biochem. J. 436 (2011) 609–620.
[19] S. Pestka, The interferons: 50 years after their discovery, there is much more to learn, J. Biol. Chem. 282 (2007) 20047–20051.
[20] S. Pestka, C.D. Krause, M.R. Walter, Interferons, interferon-like cytokines, and their receptors, Immunol. Rev. 202 (2004) 8–32.
[21] C. Bogdan, The function of type I interferons in antimicrobial immunity, Curr. Opin. Immunol. 12 (2000) 419–424.
[22] S.M. Altmann, M.T. Mellon, D.L. Distel, C.H. Kim, Molecular and functional analysis of an interferon gene from the zebrafish, Danio rerio, J. Virol. 77 (2003) 1992–2002.
[23] G. Lutfalla, H.R. Crollius, N. Stange-thomann, O. Jaillon, K. Mogensen, D. Monneron, Comparative genomic analysis reveals independent expansion of a lineage-specific gene family in vertebrates: the class II cytokine receptors and their ligands in mammals and fish, BMC Genomics 4 (2003) 29.
[24] B. Robertsen, The interferon system of teleost fish, Fish Shellfish Immunol. 20 (2006) 172–191.
[25] J.M. Gonzalez-Navajas, J. Lee, M. David, E. Raz, Immunomodulatory functions of type I interferons, Nat. Rev. Immunol. 12 (2012) 125–135.
[26] K.M. Monroe, S.M. McWhirter, R.E. Vance, Induction of type I interferons by bacteria, Cell. An. Microbiol. 12 (2010) 881–890.
[27] A. Kaplan, M.W. Lee, A.J. Wolf, J.J. Limon, C.A. Becker, M. Ding, R. Murali, E.Y. Lee, G.Y. Liu, G.C. Wong, D.M. Underhill, Direct antimicrobial activity of IFN-β, J. Immunol. 198 (2017) 4036–4045.
[28] S. Mounika, N. Jagannathan, Murali, Association of *Streptococcus* mutants and *Streptococcus sanguis* in act of dental caries, J. Pharm. Sci. Res. 7 (2015) 764–766.
[29] C. Goerke, S. Campana, M.G. Bayer, G. Döring, K. Botzenhart, C. Wolz, Direct quantitative transcript analysis of the agr regulon of *Staphylococcus aureus* during human infection in comparison to the expression profile in vitro, Infect. Immun. 68 (2000) 1304–1311.
[30] V. Cázares-Domínguez, S.A. Ochoa, A. Cruz-Córdova, G.E. Rodea, G. Escalona, A.L. Olivares, J. Olivares-Trejo Jde, N. Velázquez-Guadarrama, J. Xicohtencatl-Cortes, Vancomycin modifies the expression of the agr system in multidrug-resistant *Staphylococcus aureus* clinical isolates, Front. Microbiol. 6 (2015) 369, http://doi.org/10.3389/fmicb.2015.00369.
[31] A. Vaishampayan, A. de Jong, D.J. Wight, J. Kok, E. Grohmann, A novel antimicrobial coating represses biofilm and virulence-related genes in methicillin-resistant *Staphylococcus aureus*, Front. Microbiol. 9 (2018) 221, http://doi.org/10.3389/fmicb.2018.00221.
[32] A. Ivan, V. Elba, W. Oliver, B. Humberto, R. Rodríguez, C. Gerardo, Antimicrobial activity and stability of short and long based arachnid synthetic peptides in the presence of commercial antibiotics, Molecules 21 (2016) 225. https://doi.org/10.3390/molecules21020225.
[33] B.J. Moncla, K. Pryke, L.C. Rohan, P.W. Graebing, Degradation of naturally occurring and engineered antimicrobial peptides by proteases, Adv. Biosci. Biotechnol. 2 (2011) 404–408.
[34] P.F. Almeida, A. Pokorny, Mechanisms of antimicrobial, cytolytic, and cell-penetrating peptides: from kinetics to thermodynamics, Biochemistry 48 (2009) 8083–8093.
[35] B. Findlay, G.G. Zhanel, F. Schweizer, Cationic amphiphiles, a new generation of antimicrobials inspired by the natural antimicrobial peptide scaffold,

Antimicrob. Agents Chemother. 54 (2010) 4049–4058.
[36] X. Bi, C. Wang, L. Ma, Y. Sun, D. Shang, Investigation of the role of tryptophan residues in cationic antimicrobial peptides to determine the mechanism of antimicrobial action, J. Appl. Microbiol. 115 (2013) 663–672.
[37] A.Y. Gahane, P. Ranjan, V. Singh, R.K. Sharma, N. Sinha, M. Sharma, R. Chaudhry, A.K. Thakur, Fmoc-phenylalanine displays antibacterial activity against Gram-positive bacteria in gel and solution phases, Soft Matter 14 (2018) 2234–2244.
[38] M. Otto, Staphylococcal biofilms, Curr. Top. Microbiol. Immunol. 322 (2008) 207–228.
[39] Y.H.E. Mohammed, H.M. Manukumar, K.P. Rakesh, C.S. Karthik, P. Mallu, H.L. Qin, Vision for medicine: *Staphylococcus aureus* biofilm war and unlocking key's for anti-biofilm drug development, Microb. Pathog. 123 (2018) 339–347.
[40] A.M.S. Figueiredo, F.A. Ferreira, C.O. Beltrame, M.F. Côrtes, The role of biofilms in persistent infections and factors involved in ica-independent biofilm development and gene regulation in *Staphylococcus aureus*, Crit. Rev. Microbiol. 43 (2017) 602–620.
[41] B. Skerlavaj, D. Romeo, R. Gennaro, Rapid membrane permeabilization and inhibition of vital functions of gram-negative bacteria by bactenecins, Infect. Immun. 58 (1990) 3724–3730.
[42] M. Scocchi, M. Mardirossian, G. Runti, M. Benincasa, Non-membrane permeabilizing modes of action of antimicrobial peptides on bacteria, Curr. Top. Med. Chem. 16 (2016) 76–88.
[43] Y. Mine, F.P. Ma, S. Lauriau, Antimicrobial peptides released by enzymatic hydrolysis of hen egg white lysozyme, J. Agric. Food Chem. 52 (2004) 1088–1094.
[44] M.R. Yeaman, N.Y. Yount, Mechanisms of antimicrobial peptide action and resistance, Pharmacol. Rev. 55 (2003) 27–55.
[45] V. Frecer, B. Ho, J.L. Ding, De novo design of potent antimicrobial peptides, Antimicrob. Agents Chemother. 48 (2004) 3349–3357.
[46] Ø. Rekdal, B.E. Haug, M. Kalaaji, H.N. Hunter, I. Lindin, I. Israelsson, T. Solstad, N. Yang, M. Brandl, D. Mantzilas, H.J. Vogel, Relative spatial positions of tryptophan and cationic residues in helical membrane-active peptides determine their cytotoxicity, J. Biol. Chem. 287 (2012) 233–244.
[47] L.L. Ling, T. Schneider, A.J. Peoples, A.L. Spoering, I. Engels, B.P. Conlon, A. Mueller, T.F. Schäberle, D.E. Hughes, S. Epstein, M. Jones, L. Lazarides, V.A. Steadman, D.R. Cohen, C.R. Felix, K.A. Fetterman, W.P. Millett, A.G. Nitti, A.M. Zullo, C. Chen, K. Lewis, A new antibiotic kills pathogen without detectable resistance, Nature 517 (2015) 455–459.
[48] C. Li, J. Zhu, Y. Wang, Y. Chen, L. Song, W. Zheng, J. Li, R. Yu, Antibacterial activity of AI-Hemocidin 2, a novel N-terminal peptide of hemoglobin purified from *Arca inflata*, Mar. Drugs 15 (2017) E205, http://doi.org/10.3390/md15070205.